# Elastic Analysis of a Cracked Ellipsoidal Inhomogeneity in an Infinite Body

**Young-Tae CHO***
*Institute of Engineering and Technology, Jeonju University*

In particle or short-fiber reinforced composites, cracking of reinforcements is a significant damage mode because the cracked reinforcements lose load carrying capacity. This paper deals with elastic stress distributions and load carrying capacity of intact and cracked ellipsoidal inhomogeneities. Three dimensional finite element analysis has been carried out on intact and cracked ellipsoidal inhomogeneities in an infinite body under uniaxial tension and pure shear. For the intact inhomogeneity, as well known as Eshelby's solution, the stress distribution is uniform in the inhomogeneity and nonuniform in the surrounding matrix. On the other hand, for the cracked inhomogeneity, the stress in the region near the crack surface is considerably released and the stress distribution becomes more complex. The average stress in the inhomogeneity represents its load carrying capacity, and the difference between the average stresses of the intact and cracked inhomogeneities indicates the loss of load carrying capacity due to cracking damage. The load carrying capacity of the cracked inhomogeneity is expressed in terms of the average stress of the intact inhomogeneity and some coefficients. It is found that a cracked inhomogeneity with high aspect ratio still maintains higher load carrying capacity.

**Key Words :** Ellipsoidal Inhomogeneity, Micromechanics, Load Carrying Capacity, Cracking Damage, Three Dimensional Finite Element Method, Elastic Stress Distribution, Aspect Ratio

## 1. Introduction

Composites which contain particles or short-fibers in a ductile matrix have already been used or have the potential as engineering material because of their good formability and machinability as well as improved mechanical properties (Logsdon and Liaw, 1986; Kamat et al., 1989; Shang and Ritchie, 1989; Kim et al., 1992; Sugimura and Suresh, 1992; Roy et al., 1992; Yu et al., 1994). In the composites, a variety of damage modes such as fracture of reinforcements, interfacial debonding between reinforcements and matrix, and cracking in matrix develop from early stage of deformation under monotonic or cyclic loads (Loretto and Konitzer, 1990; Bayha et al., 1992; Llorca et al., 1993; Whitehouse and Clyne, 1993; Tohgo et al., 1996a). The observed damage modes depend on the combination of the mechanical properties of the constituents and the in-situ interfacial strength between them. In the particle or short-fiber reinforced composites, for example, both the fracture of reinforcements and interfacial debonding may be main damage modes. These damage modes reduce the tensile strength and fatigue strength because the reinforcing effect of the intact reinforcements turns into the weakening effect due to damage. On the contrary, the damage around a crack tip might be available as the toughening mechanism due to energy dissipation. The mechanical performance of the composites strongly depends on the damage mode, damage process and damage accumulation. In order to extend the application of the

* **E-mail** : dgycho@jeonju.ac.kr
**TEL** : +82-63-220-2790; **FAX** : +82-63-220-2750
Institute of Engineering and Technology, Jeonju University, #1200, Hyoja-dong 3-ga, Wansan-ku, Jeonju, Chonbuk 560-759, Korea.(Manuscript **Received** September 21, 2000 ; **Revised** March 9, 2001)

composites and to develop a new composite system, an understanding of the micromechanism of damage process in the composites is essential and micromechanics to describe the damage process should be established.

For the debonding damage of the particle-reinforced composites, Tohgo et al. developed an incremental damage theory based on the Eshelby's equivalent inclusion method (Eshelby, 1957) and Mori and Tanaka's mean field concept (Mori and Tanaka, 1973), and showed that the influence of the debonding damage on the stress-strain response of the composite is very drastic (Tohgo and Weng, 1994; Tohgo and Chou, 1996; Tohgo et al., 1996b). On the other hand, the theory for the cracking damage in the composites is also necessary, since the cracking of the reinforcement is well observed in the actual composite, particularly, short-fiber reinforced composites. Many theories for particle or short-fiber reinforced composites were established based on the Eshelby's solution for an ellipsoidal inhomogeneity in an infinite body (Mura, 1982; Arsenault and Taya, 1987; Tandon and Weng, 1988; Tohgo and Weng, 1994; Tohgo et al., 1996a, 1996b). However, the corresponding solution for a cracked ellipsoidal inhomogeneity has not been reported. Therefore, it is impossible to construct the theory of the composite containing cracking damage in the same scheme. Unit cell analyses due to finite element method have been carried out in order to investigate the influence of the debonding damage or cracking damage on the stress-strain response of the composites (Needleman, 1987; Bao, 1992; Finot et al., 1994; Brockenbrough and Zok, 1995). However, because it is assumed in the unit cell analyses that all reinforcements are in the same stage of damage process, we cannot obtain the overall stress-strain relation of a realistic composite containing intact and damaged reinforcements.

The present work has been carried out as a fundamental investigation to establish the theory for the cracking damage in the composites. Elastic stress distributions and load carrying capacity of intact and cracked ellipsoidal inhomogeneities embedded in an infinite body are analyzed based on three dimensional finite element method. Loss of the load carrying capacity of inhomogeneity due to the cracking damage is discussed from viewpoints of an aspect ratio of inhomogeneity and the combination in the elastic moduli of inhomogeneity and matrix.

## 2. Load Carrying Capacity of an Damaged Ellipsoidal Inhomogeneity

Load carrying capacity of an ellipsoidal inhomogeneity embedded in an infinite body can be defined by its average stress. High average stress comparing with the remote applied stress means high load carrying capacity of the inhomogeneity. On the other hand, when the average stress is reduced by the debonding or cracking damage of the inhomogeneity, the load carrying capacity is also reduced, and the stress free in a void means that the load carrying capacity of the void is equal to zero.

In this section, the load carrying capacity of intact and cracked inhomogeneities in an infinite body subjected to the remote applied stress as shown in Fig. 1 is discussed.

Figure 1(b) shows an intact ellipsoidal inhomogeneity embedded in an infinite body under applied stress $\sigma$. The elastic stiffness tensor of the infinite body (matrix) and the inhomogeneity are denoted by $L_0$ and $L_1$, respectively. The stress of the ellipsoidal inhomogeneity $\sigma^p$ is uniform and given by the Eshelby's equivalent inclusion method as well known (Eshelby, 1957).

$$\sigma^p = L_0(S-I)[(L_1-L_0)S+L_0]^{-1}L_1(S-I)L_0^{-1}\sigma \tag{1}$$

where $S$ is Eshelby's tensor which is expressed as a function of shape of the inhomogeneity and Poisson's ratio of the matrix, and $I$ is the identity tensor.

For an ellipsoidal inhomogeneity cracked in the cross section of xy-plane as shown in Fig. 1 (a), the stress distribution in the inhomogeneity seems to be complex and its solution have not been reported as far as the authors traced references. Figure 1 shows the principle of superposition for a cracked ellipsoidal

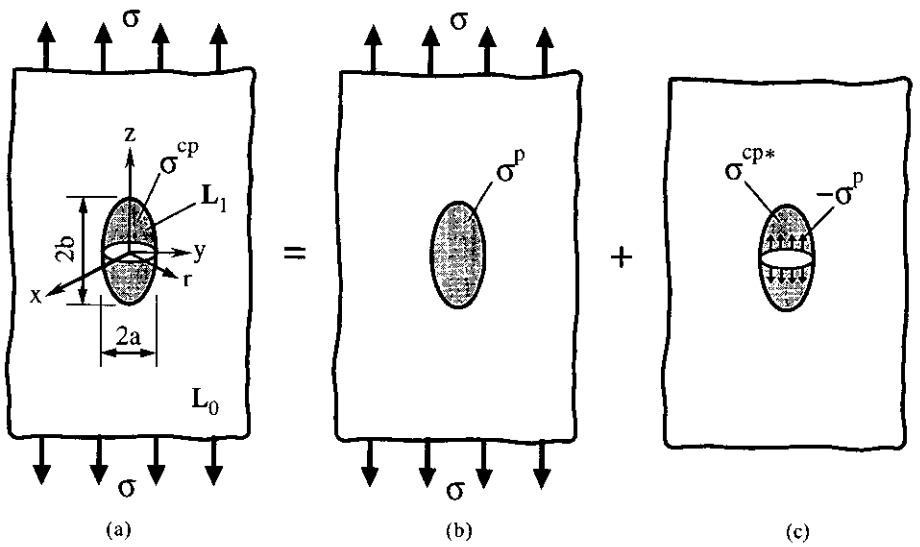


**Fig. 1** Principle of superposition for a cracked ellipsoidal inhomogeneity in infinite body

inhomogeneity in an infinite body. The stress state in the cracked inhomogeneity $\boldsymbol{\sigma}^{cp}$ is given by the sum of the stresses $\boldsymbol{\sigma}^{p}$ and $\boldsymbol{\sigma}^{cp*}$, where $\boldsymbol{\sigma}^{p}$ is the stress in the intact inhomogeneity under the applied stress $\boldsymbol{\sigma}$ and $\boldsymbol{\sigma}^{cp*}$, is the stress in the cracked inhomogeneity subjected to internal stress $-\boldsymbol{\sigma}^{p}$ on the crack surface. Therefore, the average stress of the broken inhomogeneity is expressed by

$$\overline{\boldsymbol{\sigma}}^{cp}=\boldsymbol{\sigma}^{p}+\overline{\boldsymbol{\sigma}}^{cp*} \tag{2}$$

Since $\overline{\boldsymbol{\sigma}}^{cp*}$ is taken as a function of the stress of the intact inhomogeneity $\boldsymbol{\sigma}^{p}$, Eq. (2) can be written as

$$\overline{\boldsymbol{\sigma}}^{cp}=\boldsymbol{\sigma}+\boldsymbol{h}\boldsymbol{\sigma}^{p}=(\boldsymbol{I}+\boldsymbol{h})\boldsymbol{\sigma}^{p}=\boldsymbol{k}\boldsymbol{\sigma}^{p} \tag{3}$$

where $\boldsymbol{h}$ is a coefficient expressing the reduction of average stress due to the cracking damage of an ellipsoidal inhomogeneity and $\boldsymbol{k}$ is the ratio of the average stresses of the cracked and intact inhomogeneities. The components of the stresses are given by

$$\boldsymbol{\sigma}^{p}=[\sigma^{p}_{x},\ \sigma^{p}_{y},\ \sigma^{p}_{z},\ \tau^{p}_{yz},\ \tau^{p}_{zx},\ \tau^{p}_{xy}] \tag{4}$$

$$\overline{\boldsymbol{\sigma}}^{cp}=[\overline{\sigma}^{cp}_{x},\ \overline{\sigma}^{cp}_{y},\ \overline{\sigma}^{cp}_{z},\ \overline{\tau}^{cp}_{yz},\ \overline{\tau}^{cp}_{zx},\ \overline{\tau}^{cp}_{xy}] \tag{5}$$

$$\overline{\boldsymbol{\sigma}}^{cp*}=[\overline{\sigma}^{cp*}_{x},\ \overline{\sigma}^{cp*}_{y},\ \overline{\sigma}^{cp*}_{z},\ \overline{\tau}^{cp*}_{yz},\ \overline{\tau}^{cp*}_{zx},\ \overline{\tau}^{cp*}_{xy}] \tag{6}$$

The average stress components in the broken inhomogeneity shown in Fig. 1(c) are $\overline{\sigma}^{cp*}_{z}$, $\overline{\sigma}^{cp*}_{x}$ and $\overline{\sigma}^{cp*}_{y}$ due to internal stress $-\sigma^{p}_{z}$ on the crack surface, $\overline{\tau}^{cp*}_{yz}$ due to $-\tau^{p}_{yz}$, and $\overline{\tau}^{cp*}_{zx}$ due to $-\tau^{p}_{zx}$. The coefficient $\boldsymbol{k}$ for the axisymmetric ellipsoidal inhomogeneity is described by

$$\boldsymbol{k}=(\boldsymbol{I}+\boldsymbol{h})=\begin{bmatrix} 1 & 0 & h_{13} & 0 & 0 & 0 \\ 0 & 1 & h_{13} & 0 & 0 & 0 \\ 0 & 0 & 1+h_{33} & 0 & 0 & 0 \\ 0 & 0 & 0 & 1+h_{44} & 0 & 0 \\ 0 & 0 & 0 & 0 & 1+h_{44} & 0 \\ 0 & 0 & 0 & 0 & 0 & 1 \end{bmatrix} \tag{7}$$

in the matrix form. Furthermore, in the case of the axisymmetric ellipsoidal inhomogeneity, the next relations are obtained.

$$h_{13}=h_{23},\ h_{44}=h_{55} \tag{8}$$

As a result, once the three components, $h_{33}$, $h_{13}$ and $h_{44}$ are obtained, the average stress, i.e. the load carrying capacity, of the cracked ellipsoidal inhomogeneity can be evaluated by the average stress of the intact inhomogeneity which is already obtained by the Eshelby's equivalent inclusion method. Out of the three components, $h_{33}$ and $h_{13}$ are determined by the analysis under uniaxial tension, and $h_{44}$ is by the analysis under pure shear.

## 3. Numerical Procedure

Elastic stress analyses of intact and cracked

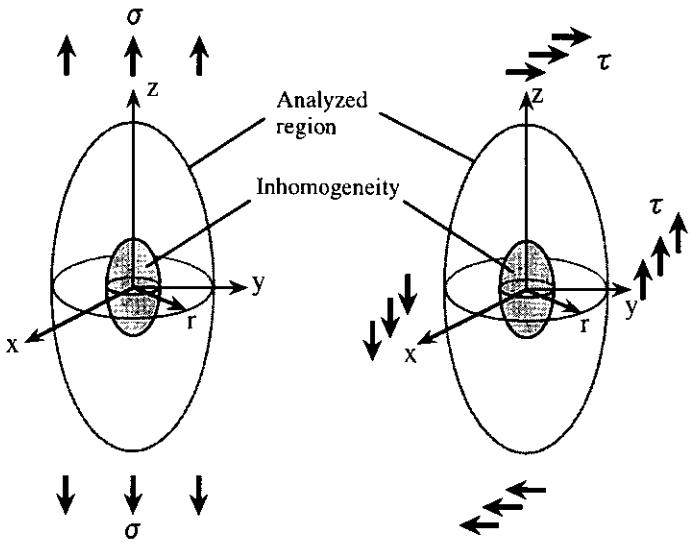


(a) An ellipsoidal inhomogeneity under uniaxial tension

(b) An ellipsoidal inhomogeneity under pure shear

**Fig. 2** Ellipsoidal inhomogeneity in infinite body under uniaxial tension and pure shear

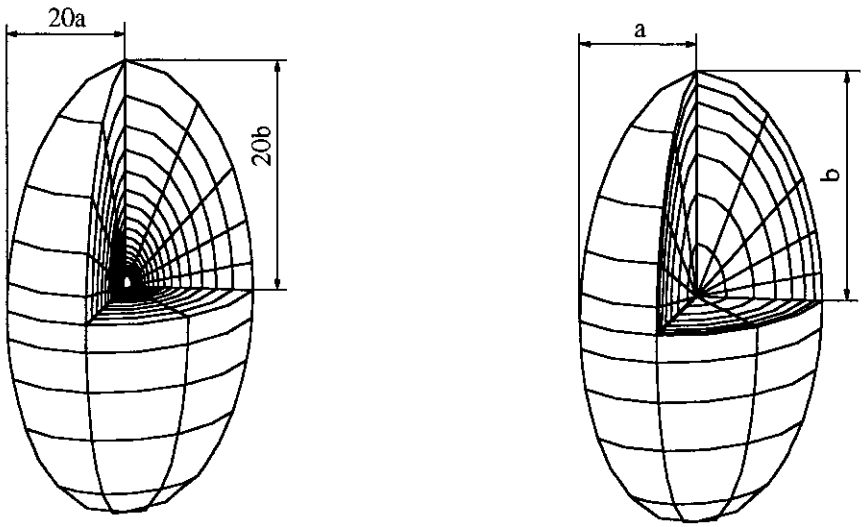


(a)

(b) Details of an inhomogeneity

**Fig. 3** Three dimensional finite element mesh used in the analysis under pure

ellipsoidal inhomogeneities embedded in an infinite body were carried out under uniaxial tension and under pure shear as shown in Figs. 2 (a) and (b). In the analyses of the ellipsoidal inhomogeneities under uniaxial tension as shown in Fig. 2(a), the axisymmetric finite element method using the quadrilateral 8-node isoparametric elements were adopted. Mesh division was carried out for a wide ellipsoidal domain including an inhomogeneity in the center, and uniaxial tensile stress $\sigma$ in the z-axis direction is applied on the surface of the domain as boundary condition (Cho et al., 1997a).

In this work, an ellipsoidal inhomogeneities under pure shear as shown in Fig. 2(b) were analyzed by the three dimensional finite element

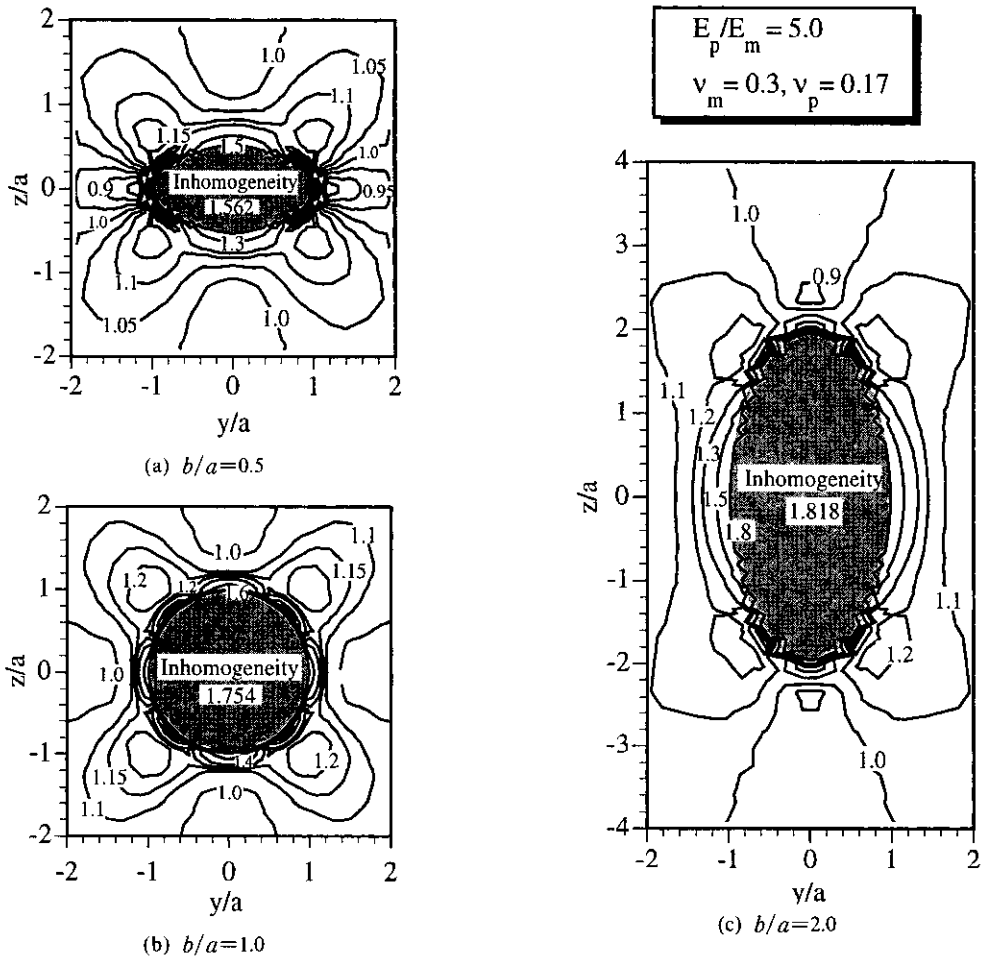


**Fig. 4** Stress distributions ($\tau_{yz}/\tau$) in and around an intact inhomogeneity under pure shear. Aspect ratios ($b/a$) of the inhomogeneity are 0.5, 1.0 and 2.0

method using the quadrilateral 20-nodes isoparametric solid elements. Mesh division was carried out for a wide ellipsoidal domain as shown in Fig. 2(b), and pure shear stress $\tau$ in the $yz$-plane is applied on the surface of the domain. An example of finite element mesh used in the elastic analysis is show in Fig. 3. Comparing with the axisymmetric mesh for the analyses under uniaxial tension, the three dimensional mesh for the analyses under pure shear became coarse because of the limitation of memory size of the computer. For the broken ellipsoidal inhomogeneity, the same mesh division with the double node points on the crack plane was used to create the stress free crack surfaces.

The size of the inhomogeneity is denoted by 2$a$ and 2$b$ in $r$ ($x$ and $y$) direction and $z$ direction, respectively. In the analyses, an aspect ratio ($b/a$) of the inhomogeneity and the combination in the elastic moduli of inhomogeneity and matrix were widely changed. The average stress in the intact and broken inhomogeneities were calculated and used as the load carrying capacity.

## 4. Numerical Results

### 4.1 Stress distribution in and around an inhomogeneity under pure shear

Stress distributions of the intact and cracked inhomogeneities are shown for the case in which Young's modulus ratio is $E_p/E_m$=5.0 and Poisson's ratios are $\nu_m$=0.3 for the matrix and

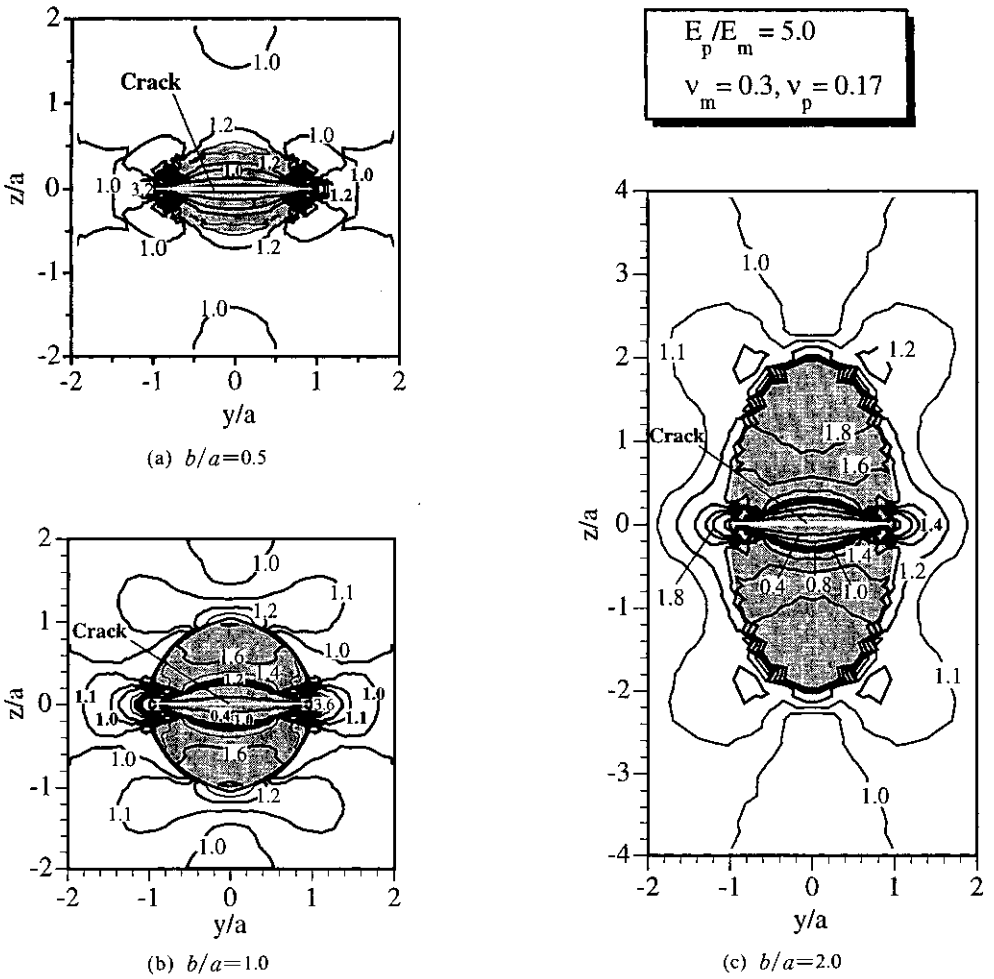


**Fig. 5** Stress distributions ($\tau_{yz}/\tau$) in and around a cracked inhomogeneity under pure shear. Aspect ratios ($b/a$) of the inhomogeneity are 0.5, 1.0 and 2.0

$\nu_p$=0.17 for the inhomogeneity. In the three dimensional analyses of the inhomogeneity under pure shear, the accuracy of the numerical results was enough for the inhomogeneities with the aspect ratio of b/a=0.5 to 2.0, but not enough for those with the high and extremely low aspect ratio because of the coarse mesh division. Therefore the results of the stress distribution are presented for the inhomogeneity with the aspect ratio of b/a= 0.5 to 2.0. Figures 4 and 5 show the distributions of the stress $\tau_{yz}$ in the $xy$-plan for the intact and cracked inhomogeneities under pure shear, respectively. The aspect ratios are 0.5 (oblate spheroid), 1.0 (sphere) and 2.0 (prolate spheroid). As shown in Fig. 4, the shear stress in the intact inhomogeneities is uniform as well known as Eshelby's solution (1957) for ellipsoidal inclusion, and nonuniform in the surrounding matrix. The maximum stress in the matrix is created in the region near the pole of the inhomogeneity. On the other hand, in the case of the cracked inhomogeneity (Fig. 5), the shear stress is released on the narrow region along the crack surface, and becomes nonuniform in the inhomogeneity, and it concentrates at the crack tip region and the pole of the inhomogeneity in the surrounding matrix.

The shear stress distributions along the $z$-axis and y-axis for the intact and broken inhomogeneities under pure shear exhibit almost the same tendency as the tensile stress distributions

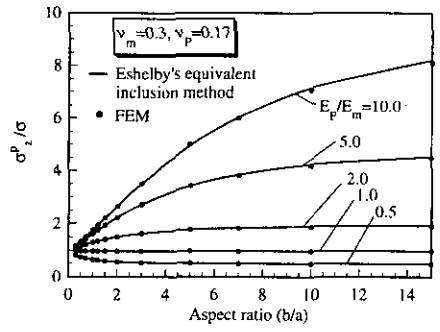


(a) Stress in $z$-axis direction

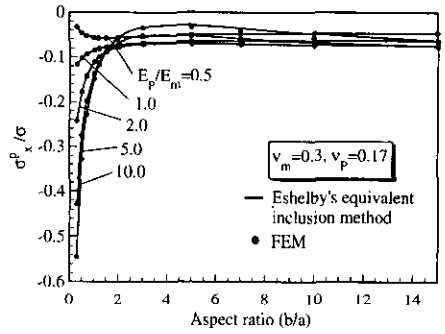


(b) Stress in $x$-axis direction

**Fig. 6** Tensile stress of an intact inhomogeneity in infinite body under uniaxial tension as a function of an aspect ratio

under uniaxial tension shown in the previous works (Cho et al., 1997a, 1997b). These distributions were obtained by the data at the Gauss points close to the z-axis and r-axis.

### 4.2 Load carrying capacity in an ellipsoidal inhomogeneity under uniaxial tension

As mentioned previously, the load carrying capacity of an ellipsoidal inhomogeneity embedded in a matrix is defined by its average stress. The average stress in the intact and cracked inhomogeneities in an infinite body under uniaxial tension is calculated based on the result of the finite element analyses, and the load carrying capacity of these inhomogeneities is discussed. In the axisymmetric finite element analysis the stress components in z-axis, radial and circumferential directions, $\overline{\sigma}^p{}_z$, $\overline{\sigma}^p{}_r$ and $\overline{\sigma}^p{}_\theta$, are obtained. Here, the stress components in the rectangular coordinate system $\overline{\sigma}^p{}_z$ and $\overline{\sigma}^p{}_x = \overline{\sigma}^p{}_y$ transferred from, $\overline{\sigma}^p{}_z$, $\overline{\sigma}^p{}_r$ and $\overline{\sigma}^p{}_\theta$ are used for the discussion.

Figures 6(a) and (b) show the stresses $\overline{\sigma}^p{}_z$ and $\overline{\sigma}^p{}_r$ of the intact inhomogeneity in an infinite body under uniaxial tension as a function of an aspect ration $(b/a)$ for various combinations in the elastic moduli of inhomogeneity and matrix. The solid lines and pilots indicate the results of Eshelby's equivalent inclusion method (Eq. (1)) and the results of the finite element analyses, respectively. Good agreement between both results shows that the present finite element analyses of the ellipsoidal domain containing the inhomogeneity in the center well simulate an inhomogeneity in an infinite body. It is found from Fig. 6(a) that with increasing the aspect ratio, the stress in tensile direction $\sigma^p{}_z$ increases for the Young's modulus ratio of $E_p/E_m > 1$, and decreases for $E_p/E_m < 1$. The stress perpendicular to tensile direction $\sigma^p{}_x$ shown in Fig. 6(b) is always negative, and it depends on the Young's modulus ratio at the region of low aspect ratio but converges to around -0.06 with increasing the aspect ratio.

As shown in the previous section, the stress in the inhomogeneity is released by the cracking damage, but the cracked inhomogeneity still has a large amount of load carrying capacity. From Eq. (3), relations between the average stresses of the cracked and intact inhomogeneities under multiaxial tension and pure shear are expressed by

$$\overline{\sigma}^{cp}{}_z = (1 + h_{33})\sigma^p{}_z \tag{9}$$

$$\overline{\sigma}^{cp}{}_x = \sigma^p{}_x + h_{13}\sigma^p{}_z \tag{10}$$

Using Eqs. (9) and (10) the coefficients h33 and h13 are determined from the numerical results of the average stresses of intact and cracked ellipsoidal inhomogeneity. Figures 7 and 8 show relationship between the coefficients $h_{33}$ and $h_{13}$, and the aspect ratio for various combinations in the elastic moduli.

### 4.3 Load carrying capacity in an ellipsoidal inhomogeneity under pure shear

The uniform stress $\tau^p{}_{yz}$ of the intact inhomogeneity in an infinite body under pure shear is shown as a function of an aspect ratio for

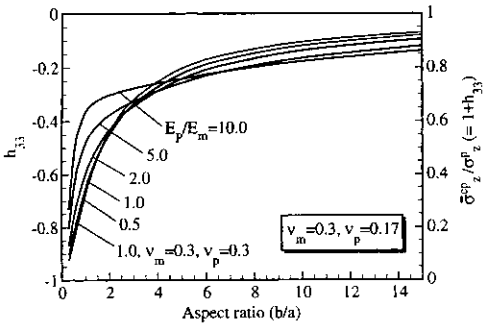


**Fig. 7** Coefficient ($h_{33}$) and ratio of load carrying capacity of cracked and intact inhomogeneities as a function of an aspect ratio

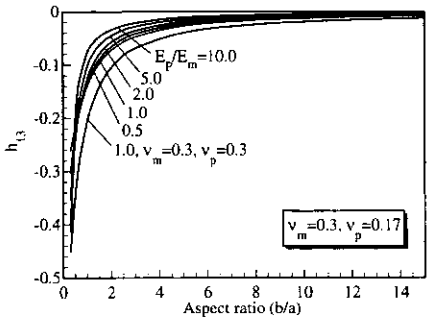


**Fig. 8** Coefficient ($h_{13}$) as a function of an aspect ratio

various combinations in the elastic moduli of inhomogeneity and matrix in Fig. 9. The numerical results shown by plots are consistent with the results of Eshelby's equivalent inclusion method shown by solid lines in the region of the aspect ratio of $b/a$=0.5 and 2.0, but the deviation between both is observed in the other region of the aspect ratio. This means that the present three dimensional finite element analyses of the ellipsoidal domain containing the inhomogeneity well simulate an inhomogeneity in an infinite body for the aspect ratio of $b/a$=0.5 to 2.0. In order to obtain the accurate numerical results for the inhomogeneities with low and high aspect ratio, the fine mesh division is necessary. It is found from Fig. 9 that with increasing the aspect ratio, the shear stress increases for the Young's modulus ratio of $E_p/E_m>1$, and decreases for $E_p/E_m<1$ up to $b/a$=1.5, and then becomes constant.

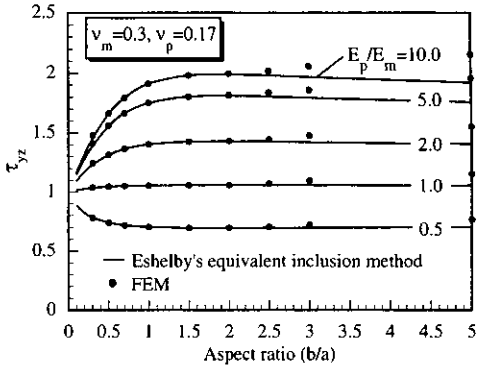


**Fig. 9** Shear stress of an intact inhomogeneity in infinite body under pure shear as a function of an aspect ratio

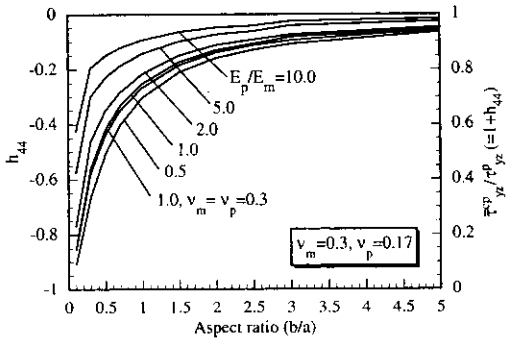


**Fig. 10** Coefficient ($h_{44}$) and load carrying capacity ratio on shear stress as a function of an aspect ratio

From Eq. (3), relation between the average stresses of the broken and intact inhomogeneities under pure shear is expressed by

$$\bar{\tau}^{cp}_{yz}=(1+h_{44})\tau^p_{yz} \tag{11}$$

The coefficient $h_{44}$ is determined based on the above equation from the numerical results of the average shear stresses. Figure 10 shows the coefficients $h_{44}$ as a function of the aspect ratio for various combinations in the elastic moduli.

## 5. Discussion

Based on the finite element analyses of the intact and cracked ellipsoidal inhomogeneities under uniaxial tension and under pure shear, three components $h_{33}$, $h_{13}$ and $h_{44}$ have been obtained as functions of the aspect ratio and the

combination of the elastic moduli. As shown in Eq. (3), once these three components are obtained, the average stress of the broken inhomogeneity can be easily evaluated in terms of the average stress of the intact inhomogeneity. Therefore, the three components $h_{33}$, $h_{13}$ and $h_{44}$ are very important.

Hereafter, we discuss in more detail the change of the load carrying capacity due to cracking damage of the ellipsoidal inhomogeneity. When Fig. 7 is observed for a scale of the right hand side, it exhibits a ratio of the load carrying capacity on tensile stress $\overline{\sigma}^{cp}{}_z/\sigma^p{}_z$ which is defined by the ratio of the average stress in the broken inhomogeneity ($\overline{\sigma}^{cp}{}_z$) to the stress in the intact inhomogeneity ($\sigma^p{}_z$). Figure 10 also exhibits a ratio of the load carrying capacity on shear stress $\overline{\tau}^{cp}{}_{yz}/\tau^p{}_{yz}$ for a scale of the right hand side. As shown in Fig. 7, the load carrying capacity ratio on tensile stress is always smaller than one, i. e. the inhomogeneity reduces its load carrying capacity by the cracking damage. It is found that the load carrying capacity ratio increases with increasing the aspect ratio and depends on the combination of the elastic moduli. The load carrying capacity ratio is equal to zero for a penny shape inhomogeneity ($b/a=0$), while it approaches to one for a continuous long fiber ($b/a=\infty$). This means that a penny shape inhomogeneity loses completely the load carrying capacity by the cracking damage while the infinitely long fiber in an infinite body never loses it. With increasing Young's modulus ratio $E_p/E_m$, the load carrying capacity ratios increase in the region of low aspect ratio and decrease in the region of high aspect ratio. Particularly, the influence of $E_p/E_m$ to the load carrying capacity is drastic for the inhomogeneity with low aspect ratio. This suggests that in a composite reinforced with ellipsoidal inhomogeneity with low aspect ratio a stiffer inhomogeneity maintains higher load carrying capacity after cracking damage. The characteristics of the load carrying capacity ratio on shear stress in Fig. 10 are almost the same as those mentioned above for Fig. 7, except for the influence of on the load carrying capacity ratio for the inhomogeneity with high aspect ratio. From the comparison of the results for two cases; $E_p/E_m=1.0$, $\nu_m=0.3$, $\nu_p=0.17$ and $E_p/E_m=1.0$, $\nu_m=\nu_p=0.3$, Figs. 7, 8 and 10, the influence of Poisson's ratio is insignificant on the load carrying capacity ratio or $h_{33}$ and $h_{44}$, and is relatively remarkable on $h_{13}$.

## 6. Conclusions

Three dimensional finite element analyses have been carried out on the elastic stress distribution and load carrying capacity of intact and cracked ellipsoidal inhomogeneities embedded in an infinite body under pure shear. Conclusions obtained from the numerical results are summarized as follows:

(1) For the intact inhomogeneity, the stress distribution is uniform in the inhomogeneity and nonuniform in the surrounding matrix, as well known as Eshelby's solution. On the other hand, for the cracked inhomogeneity, the stress in the region near the crack surface in the inhomogeneity is considerably released and the stress distribution becomes more complex.

(2) The average stress in the cracked inhomogeneity is expressed by the average stress of the intact inhomogeneity based on the numerical results.

(3) The inhomogeneity in an infinite body loses load carrying capacity by cracking damage, but the cracked inhomogeneity still maintains it to some extent.

(4) The ratio of the load carrying capacity of the intact and cracked inhomogeneities is given as a function of the aspect ratio of the inhomogeneity. It is found that the cracked inhomogeneity with higher aspect ratio maintains higher load carrying capacity than one with low aspect ratio.

## References

Arsenault, R. J. and Taya, M., 1987, "Thermal Residual Stress in Metal Matrix Composite," *Acta Metall.*, Vol. 35, No. 3, pp. 651~659.

Bao, G., 1992, "Damage due to Fracture of Brittle Reinforcements in a Ductile Matrix," *Acta*

*Metall. Mater.*, Vol. 40, No. 10, pp. 2547~2555.

Bayha, T. D., Kilmer, R. J. and Wawner, F. E., 1992, "The Fracture Characteristics of Al-9Ti/SiCp Metal Matrix Composites," *Metall. Trans. A.*, Vol. 23A, pp. 1653~1662.

Brockenbrough, J. R. and Zok, F. W., 1995, "On the Role of Particle Cracking in Flow and Fracture of Metal Matrix Composites", *Acta Metall. Mater.*, Vol. 43, No. 1, pp. 11~20.

Cho, Y. -T, Tohgo, K. and Ishii, H., 1997a, "Finite Element Analysis of a Cracked Ellipsoidal Inhomogeneity in an Infinite Body and Its Load Carrying Capacity," *JSME Int. J.*, Ser. A, Vol. 40, No. 3, pp. 234~241.

Cho, Y. -T, Tohgo, K. and Ishii, H., 1997b, "Load Carrying Capacity of a Broken Ellipsoidal Inhomogeneity," *Acta Mater.*, Vol. 45, pp. 4787~4795.

Eshelby, J. D., 1957, "The determination of the Elastic Field of an Ellipsoidal Inclusion, and Related Problems," *Proc. Royal Society*, London, Vol. A241, pp. 376~396.

Finot, M., Shen, Y. -L., Needleman, A. and Suresh, S., 1994, "Micromechanical Modeling of Reinforcement Fracture in Particle-Reinforced Metal-Matrix Composite," *Metall. Trans. A*, Vol. 25A, pp. 2403~2420.

Kamat, S. V., Hirth, J. P. and Mehrabian, R., 1989, "Mechanical Properties of Particulate-Reinforced Aluminum-Matrix Composites," *Acta Metall.*, Vol. 37, No. 9, pp. 2395~2402.

Kim, H. J., Iwanari, H., Yoon, E. P. and Kobayashi, T., 1992, "Effect of Particle Volume Fraction on Fracture of SiC/6061 Al Composites," *J. Mater. Sci. . Letters*, Vol. 11, pp. 950~952.

Llorca, J., Martin, A., Ruiz, J. and Elices, M., 1993, "Particulate Fracture during Deformation of a Spray Formed Metal-Matrix Composite," *Metall. Trans. A*, Vol. 24A, pp. 1575~1588.

Logsdon, W. A. and Liaw, P. K., 1986, "Tensile Fracture Toughness and Fatigue Crack Growth Rate Properties of Silicon Carbide Whisker and Particulate Reinforced Aluminum Metal Matrix Composites," *Engng Fracture Mech.*, Vol. 24, No. 5, pp. 737~751.

Loretto, M. H. and Konitzer, D. G., 1990, "The Effect of Matrix Reinforcement Reaction on Fracture in Ti-6Al-4V-Base Composites," *Metall. Trans. A*, Vol. 21A, pp. 1579~1587.

Mori, T. and Tanaka, K., 1973, "Average Stress in Matrix and Average Elastic Energy of materials with misfitting Inclusions," *Acta Met.*, Vol. 21, pp. 571~574.

Mura, T., 1982, Micromechanics of Defects in Solids, Martinus Nijhoff, The Hague.

Needleman, A., 1987, "A Continuum Model for Void Nucleation by Inclusion Debonding," *Trans. ASME, J. Appl. Mech.*, Vol. 54, pp. 525~531.

Roy, M., Venkataraman, B., Bhanuprasad, V. V., Mahajan, Y. R. and Sundararajan, G., 1992, "The Effect of Particulate Reinforcement on the Sliding Wear Behavior of Aluminum Matrix Composites," *Metall. Trans. A*, Vol. 23A, pp. 2833~2847.

Shang, J. K. and Ritchie, R. O., 1989, "Crack Bridging by Uncracked Ligaments during Fatigue-Crack Growth in SiC-Reinforcement Aluminum-Alloy Composite," *Metall. Trans. A, Vol. 20A*, pp. 897~908.

Sugimura, Y. and Suresh, S., 1992, "Effects of SiC Content on Fatigue Crack Growth in Aluminum Alloys Reinforced with SiC Particles," *Metall. Trans. A*, Vol. 23A, pp. 2231~2242.

Tandon, G. P. and Weng, G. J., 1988, "A Theory of Particle-Reinforced Plasticity," *ASME, J. Appl. Mech.*, Vol. 55, pp. 126~135.

Tohgo, K. and Weng, G. J., 1994, "A Progressive Damage Mechanics in Particle-Reinforced Metal-Matrix Composites under High Triaxial Tension," *ASME J. Eng. Mat. Tech.*, Vol. 116, pp. 414~420.

Tohgo, K. and Chou, T. W., 1996, "Incremental Theory of Particulate-Reinforced Composites Including Debonding Damage," *JSME Int. J.*, Ser. A, Vol. 39, No. 3, pp. 389~397.

Tohgo, K., Mochizuki, K., Takahashi, H. and Ishii, H., 1996a, "Application of Incremental Damage Theory to Glass Particle Reinforced Nylon 66 Composites," *Localized Damage IV, Computer-Aided Assessment and Control, Com-*

*putational Mechanics Publications*, pp. 351~358.

Tohgo, K., Suzuki, N. and Ishii, H., 1996b, "Influence of Debonding Damage on a Crack Tip Field in Particulate-Reinforced Ductile-Matrix Composite," *Int. J. Damage Mech.*, Vol. 5, pp. 150~170.

Whitehouse, A. F. and Clyne, T. W., 1993, "Cavity Formation during Tensile Straining of Particulate and Short Fiber Metal Matrix Composite," *Acta Metall. Mater.*, Vol. 41, No. 6, pp. 1701~1711.

Yu, S. -Y., Ishii, H. and Tohgo, K., 1994, "Corrosion Fatigue of SiC Whisker or SiC Particulate Reinforced 6061 Aluminum Alloy," *Fatigue Fract. Engng Mater. and Struct.*, Vol. 17, No. 5, pp. 571~578.